

# Implementation of geant4 application for tomography emission Monte Carlo Code in the calculation of dose distribution in external radiation therapy

A.B. Yeke Dehghan<sup>1</sup>, A. Mostaar<sup>1,2\*</sup>, P. Azadeh<sup>3</sup>

<sup>1</sup>Department of Medical Physics and Biomedical Engineering, School of Medicine, Shahid Beheshti University of Medical Sciences, Tehran, Iran

<sup>2</sup>Radiation Biology Research Center, Iran University of Medical Sciences, Tehran, Iran

<sup>3</sup>Department of Radiation Oncology, School of Medicine, Shahid Beheshti University of Medical Sciences, Tehran, Iran

## ABSTRACT

### ► Original article

**\*Corresponding author:**

Ahmad Mostaar, Ph.D.,

E-mail: [mostaar@sbmu.ac.ir](mailto:mostaar@sbmu.ac.ir)

Received: December 2022

Final revised: March 2023

Accepted: May 2023

Int. J. Radiat. Res., October 2023;  
21(4): 663-673

DOI: 10.52547/ijrr.21.4.9

**Keywords:** GATE, geant4, Monte Carlo Code, photon beam.

**Background:** The "Geant4 Application for Tomography Emission" (GATE) toolkit comprises advanced open-source Monte Carlo (MC) code for use in medical imaging and radiotherapy simulations. This study aimed to verify the GATE toolkit results against a water phantom and then to show the dose calculation capabilities of the GATE for radiotherapy. The results were compared with three dose calculation algorithms using patients' Computerized Tomography (CT) data. **Materials and Methods:** A Linac with a 6 MV photon beam was simulated in the GATE code. The code was verified, head CT images of three patients were inserted into the GATE as realistic phantoms, and simulations were performed for different field sizes and angles. The Percent Depth Doses (PDDs) and transverse profiles were extracted from the GATE simulation and calculation algorithms. Their results were compared regarding the Dose Difference (DD) and gamma index for the PDDs and the Full Width at Half Maximum (FWHM) for the profiles. **Results:** Using the patient CT data for the PDDs, the gamma pass rate with 3%/3 mm criteria in the comparison between the GATE simulation and algorithms for all fields ranged from 89.4% to 98.8%, with an average of 92.8%. The extracted FWHMs from the GATE and algorithms were in good agreement, and their differences ranged from 0.1 to 1.2 mm. **Conclusions:** The GATE MC toolkit has good potential for implementation in radiotherapy Treatment Planning Systems (TPS) for dose calculations.

## INTRODUCTION

The Monte Carlo (MC) simulation is an important research method in nuclear medicine, radiology, and radiotherapy (1-3). It is one of the most accurate methods for dose calculation and assessment. Therefore, MC simulations can evaluate and verify other dose-calculation algorithms (4-6). The MC simulation techniques have certain advantages and drawbacks; for example, they can model both electron transport and photon scattering in a desired material (7-10), but their main drawback is the long computational time, especially for dosimetry applications (11). In an MC simulation, all materials, anatomical geometries, modalities, and devices can be modeled accurately and used for precise estimations of quantities (12). Different codes are currently dedicated to dosimetry and radiotherapy applications and are classified into groups (13-15). As a user-friendly and open-source MC simulation platform, the "Geant4 Application for Emission Tomography" (GATE) allows a user to simulate

combined imaging, radiotherapy, and dosimetry studies (1, 16-19). GATE v6.0 provides users with new tools to walk through the radiation therapy simulation field (20). This MC platform shows considerable properties that are either inherited from GEANT4 or have been additionally developed, such as simulating voxelized sources and phantoms, and time-dependent phenomena, such as source decays and volume movements (13). Moreover, users can simulate the dose distribution in a phantom during radiation therapy (21). Sarit *et al.* (1) assessed the applicability of the GATE.

Dose calculation algorithms are the most important component of modern Treatment Planning Systems (TPSs). The International Commission on Radiation Units & Measurements recommends that the error of the delivered dose be less than 5% (10, 22). This means that each part of the treatment (machine calibration, patient setup, dose calculation, and dose delivery) must be performed as accurately as possible, i.e., with an error of less than 5%. The required accuracy for the dose calculation should be

2–3% (10, 23, 24). The accuracy of the calculated dose distribution significantly influences the precision and reliability of radiotherapy treatment plans (25, 26). Generally, treatment planning systems include several algorithms with limited accuracy in dose calculations. One of the most important disadvantages of these dose calculation algorithms is that they cannot appropriately consider the changes in electron transport at the border between two media with low- or high-density, such as lung or bone tissues. Thus, they show significant errors in those regions (10% or more); this remains a challenge for certain treatment planning systems (27, 28). Several authors investigated this issue for different dose calculation algorithms (5, 24, 29–31).

Using Computed Tomography (CT) scan images, a heterogeneous phantom can be defined with several tissues with different densities. The GATE MC code can read the CT scan images of a patient and allow the user to insert the images as voxelized geometries to present anatomical specifications of the patient, e.g., for reading attenuation maps (2, 21). Users can utilize a method known as stoichiometric calibration to generate a relationship between the Hounsfield Units (HU, the voxel values) and the mass density of each voxel according to a list of predetermined materials (2). Schneider *et al.* (32) proposed a method for converting CT data to density data for MC simulations based on a stoichiometric calibration technique and considered 71 human tissues (33). The automated HU stoichiometric calibration method is used in the GATE (18).

The MC codes, such as EGSnrc/BEAMnrc, are currently validated for radiation therapy applications (34). Jan *et al.* (20) used CT images for radiotherapy simulations, but their main goal was to show the potential of the GATE for complex simulations; they did not compare their results with any dose calculation algorithms or measurement data. Accordingly, the present study aimed to evaluate and verify the GATE toolkit by comparison with dose distribution measurements in a water phantom. Subsequently, the GATE simulation outputs performed with patients' head CT data as a heterogeneous medium were compared with those of three commercial dose calculation algorithms to show the GATE's dose calculation capability.

This study's novelty is using the patient's CT data as a voxelized phantom, unlike most other research using data from artificial phantoms to implement simulation in GATE. Despite being a very time-consuming procedure, we also used results in .mhd/.raw format as recommended in the manual.

## MATERIALS AND METHODS

In this study, the GATE v8.0 toolkit and three patients' head CT (Siemens, Somatom, Erlangen,

Germany) images were used to evaluate and validate the performance of the toolkit in radiotherapy studies. According to the features of this toolkit, users can insert CT data in a proper format as a voxelized phantom for realistic simulation. The process of this work consisted of five steps: (a) GATE toolkit benchmarking, (b) GATE toolkit verification against the water phantom, (c) GATE simulations for three patients based on CT data, (d) creating treatment plans in TPS for the three patients corresponding to the plans used in the GATE, and (e) comparing the results from the GATE simulation with outputs from created plans for the three patients in the TPS.

A linear accelerator (Compact model, Elekta, Stockholm, Sweden) was simulated according to the manufacturer's specifications. This simulation was divided into two parts: (a) a patient-independent part containing the target, primary collimator, flattening filter, monitor ion chamber, and mirror, and (b) a patient-dependent part containing secondary collimator jaws and the water phantom (used for verification) or voxelized phantom (used for patient simulations). To define the photon source, a thin cylindrical volume was positioned between parts (a) and (b), and then a phase-space actor was attached to the thin cylindrical volume. The phase space actor recorded the information of photons entering into the volume (such as their energy and direction), and a phase space file was created. Figure 1 shows a schematic model of the 6-MV linear accelerator head as simulated in the GATE and the location of the phase-space plane. The generated phase space file was used as a photon point source placed 100 cm away from the surface of the water phantom and used to verify the GATE toolkit.

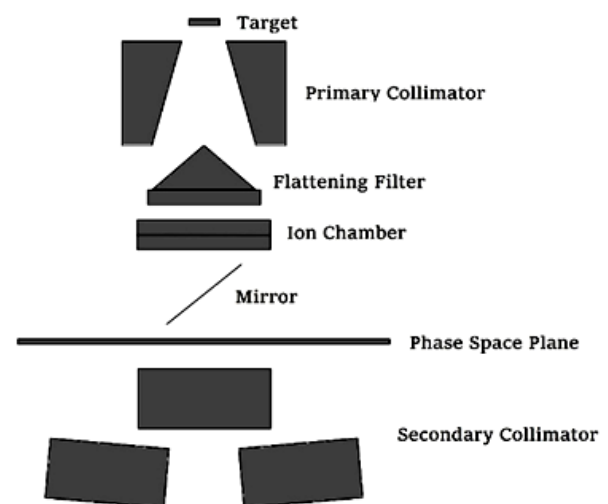


**Figure 1.** Schematic model of the 6-MV linear accelerator head simulated in the Geant4 Application for Tomography Emission (GATE) and location of the phase space plane.

### Benchmarking of the Geant4 application for tomography emission toolkit

The electron source specified the spectrum of the photon beam, and the energy of the electrons was

benchmarked by comparing the GATE simulations and measurements in a water phantom <sup>(35)</sup>. The measurements and simulations were conducted in a  $10 \times 10 \text{ cm}^2$  field size.

### Verification of the GATE toolkit

The GATE MC simulation was verified based on the dosimetric data entered into the TPS, such as the Percentage Depth Dose (PDD) and dose profiles. These data were measured using the MP3 water phantom (PTW, Freiburg, Germany) and a Semiflex ion chamber ( $0.125 \text{ cm}^3$ , PTW, Freiburg, Germany). In contrast, a  $40 \times 30 \times 40 \text{ cm}^3$  water phantom was modeled using the GATE code. The verification process was conducted by comparing the measurements, simulation PDDs, and transverse profiles extracted from  $6 \times 6$ ,  $10 \times 10$ , and  $20 \times 20 \text{ cm}^2$  field sizes in terms of Dose Difference (DD)/gamma index and dose difference/Full Width at Half Maximum (FWHM), respectively.

### Simulation based on patients' computerized tomography images

To compare the GATE toolkit with calculation algorithms after benchmarking and verification steps, simulations for dose distributions were conducted based on head CT images in the Digital Imaging and Communications in Medicine (DICOM) format for three patients. First, the simulation was performed with different field sizes and specific radiation angles for each patient, and then the same plan was created in the TPS according to the simulation information. After the completion of the simulation, the outputs from the simulation and TPS were extracted for comparison. The dose prescription for all three patients was 54 Gy in 27 fractions, meaning the dose per fraction of 2 Gy. Two similar  $4 \times 4 \text{ cm}^2$  fields at  $90^\circ$  and  $270^\circ$  and isocenter depths of 28 and 104 mm were used for the first patient, respectively. For the second patient, four fields with a  $5.5 \times 5.5 \text{ cm}^2$  field size at  $0^\circ$ ,  $90^\circ$ ,  $180^\circ$ , and  $270^\circ$  and isocenter depths of 94, 86, 72, and 78 mm were used, respectively. Finally, for the third patient, three fields with field sizes of  $5 \times 6$ ,  $6 \times 6$ , and  $7 \times 6 \text{ cm}^2$  at  $60^\circ$ ,  $180^\circ$ , and  $300^\circ$  and isocenter depths of 58, 76, and 90 mm were defined, respectively. All nine fields were exclusive and had distinct isocenter depths. The CT images of the patients in the DICOM format were converted to the required format (.mhd/.raw as recommended in the GATE manual) using VV 4D-slicer software (<https://www.creatis.insa-lyon.fr/rio/vv>) <sup>(21)</sup>. The VV is an open-source software to open and convert a DICOM image to a different format, such as Analyze or MetaImage <sup>(36)</sup>. The value of each voxel was converted to a density using the automated HU stoichiometric calibration method, and a voxelized phantom was generated, as shown in figure 2. One of the most important parts of this method was the definition of two files, as it created a

relationship between the voxel values and density. For instance, the effect of the headrest used in the CT scan process on the dose distribution in the voxelized phantom of the patient decreased significantly by defining its density as close to that of air. Notably, these changes could affect some tissues whose density values were close to that of the headrest. Therefore, the density range and tolerance needed to be defined accurately.

The range cutoff was defined as 1 mm, which was considered half of the output voxel size. Other volumes inherited the range cutoff from their mother's volume (i.e., world). A "Dose Actor" tool was used to obtain the dose distributions. This actor is attached to voxelized geometries and stores information into 3D matrices, such as the energy deposited ( $e_{\text{dep}}$ ), dose deposited, dose uncertainty,  $e_{\text{dep}}$  uncertainty, number of hits, and squared dose. In this study, the doses and dose uncertainties were extracted. The voxel size of the output 3D matrices was set to  $2 \times 2 \times 2 \text{ mm}^3$  (matrix resolution), and the output was saved in the .mhd/.raw format. The dose distribution outputs were opened using the VV software, and the PDDs for the central axis and transverse profiles for the isocenter depth were extracted. The number of primaries for the GATE verification was set to  $1.5 \times 10^9$  for  $6 \times 6 \text{ cm}^2$  and  $10 \times 10 \text{ cm}^2$  and  $4 \times 10^9$  for a field size of  $20 \times 20 \text{ cm}^2$ , and the simulation with the CT data was set to  $1 \times 10^9$ . The simulation with CT data took time approximately 7.5 to 15 times longer than the verification step in which a homogeneous water phantom was simulated. A system with a 3 GHz Xeon CPU carried out the simulations, and each simulation with CT data needed at least 15 days to achieve the desired results with acceptable uncertainty. In contrast, for the verification step, the run times of the simulations were approximately 24–48 hours.

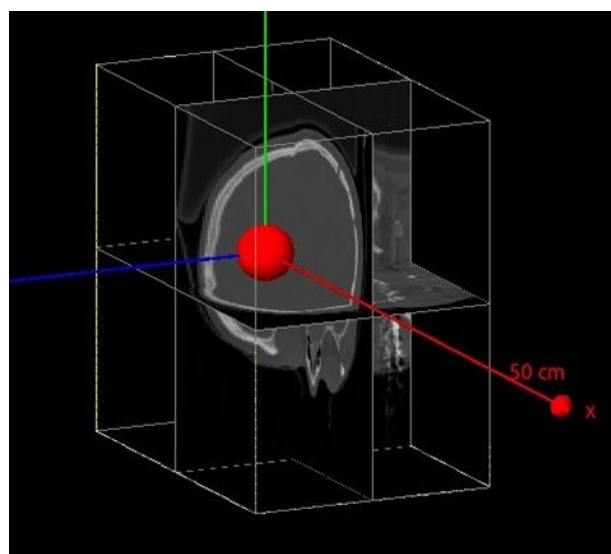


**Figure 2.** Voxelized phantom generated based on a patient's computerized tomography (CT) images (image captured in "qt" mode).

### Creating a plan in the treatment planning system

The CT images of the patients were imported into the Isogray TPS (Version 4.2.3.63L, Dosisoft, Cachan, France). This TPS had three dose calculation algorithms: Collapsed Cone Convolution (CCC), Convolution Fast Fourier Transform (CFFT), and Clarkson (CLKS). Plans with the same parameters as in the GATE simulations, such as the field size, beam angle, and source-to-skin distance, were created in the TPS for each patient. The photon beams were 6 MV for all plans, and the dose calculations were performed for the same dose prescription in the GATE simulation. Finally, the doses calculated by the TPS were extracted as 3D matrices comprising  $2 \times 2 \times 2$  mm<sup>3</sup> voxels for all beams and the three aforementioned algorithms.

### Comparing the GATE toolkit and algorithms' outputs

The PDDs and transverse profiles were extracted from the TPS and GATE simulation outputs using the VV software to compare the GATE toolkit and algorithm results. The PDDs were extracted from the beam's central axis, and the transverse profiles were extracted from the isocenter depth in the central plane of the beam. The outputs were compared regarding the dose difference and gamma index for the PDDs and the FWHM terms for the transverse profiles. The dose difference was calculated using equation (1).

$$\Delta D = 100 \times \frac{|D_{ref} - D_{eva}|}{D_{ref}} \quad (1)$$

In equation (1),  $D_{ref}$  is the dose calculated by the GATE, and  $D_{eva}$  is the dose calculated by the TPS. In a broad beam, the FWHM of the transverse profile at the isocenter represents the size of the geometrical field. Therefore, calculating the FWHM is a general method for verifying the field size<sup>(37)</sup>. All the extracted PDDs and profiles were normalized to the maximum dose. In addition, the doses calculated by TPS and the GATE simulations in the form of the

PDDs and profiles were compared in terms of the 1D gamma index for all beams and the three dose calculation algorithms. The gamma evaluation proposed by Low *et al.*<sup>(38)</sup> is one of the most important methods for evaluating the calculated dose distributions in complex modalities. This metric combines the dose difference and distance-to-agreement (DTA) criteria<sup>(39)</sup>. The agreement rate of the two dose distributions depends on a predefined percentage of gamma ( $\gamma$ ) value between 0 and 1. If the gamma index is greater than one, it indicates a failure result in the comparison. Each participant's part in the gamma index, i.e., the DD and DTA, must be predefined. These are commonly determined as 2%/2mm, 3%/3 mm, or 5%/5 mm, respectively. In addition, the percentage of points with a gamma value lower than or equal to one is defined as the pass rate. This study determined the DD and DTA criteria in the gamma index as 2%/2 mm for the verification step and 3%/3 mm for the patients' data analysis. The gamma function was used to analyze the data in this study using a software package called Gnuplot (<https://sourceforge.net/projects/gnuplot>)<sup>(40)</sup>.

## RESULTS

### GATE toolkit verification

The mean dose differences between the GATE simulations and measurements in the water phantom were 0.7%, 0.8%, and 1.3% for the  $6 \times 6$ ,  $10 \times 10$ , and  $20 \times 20$  cm<sup>2</sup> field sizes, respectively, and the maximum dose difference occurring at a depth of zero for all three fields was 8.2%, 7.4%, and 12.8%. The PDDs extracted from the measurements and simulations for the  $6 \times 6$ ,  $10 \times 10$ , and  $20 \times 20$  cm<sup>2</sup> field sizes are compared in figure 3. In addition, the gamma pass rates considering the 2%/2-mm criteria for the  $6 \times 6$ ,  $10 \times 10$ , and  $20 \times 20$  cm<sup>2</sup> field sizes were 100.0%, 98.4% and 90.4%, respectively. The value with the criterion of 3%/3 mm for the three field sizes was 100%.

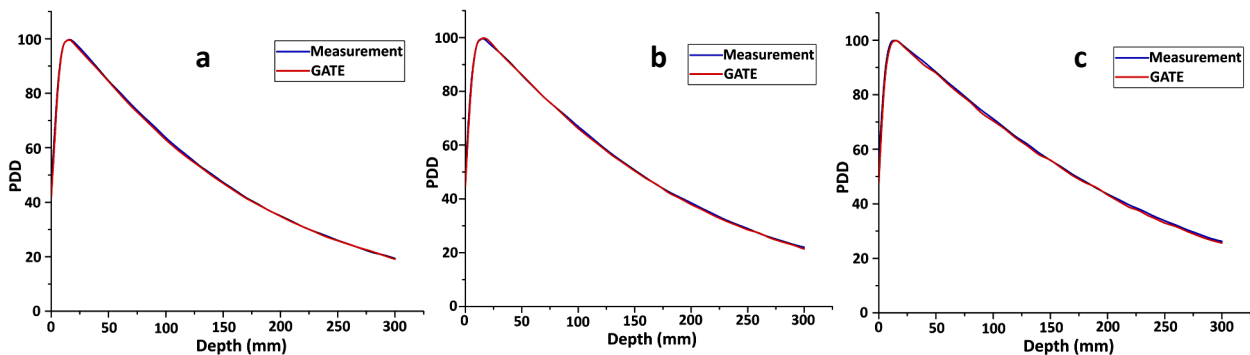


**Figure 3.** Comparison of percent depth dose (PDDs) between GATE simulations and measurements in (a)  $6 \times 6$  cm<sup>2</sup> (b)  $10 \times 10$  cm<sup>2</sup>, and (c)  $20 \times 20$  cm<sup>2</sup> field sizes.

The transverse profiles, as proposed by Venselaar *et al.* (41), were assessed in three regions: (1) the flat region inside the field, (2) the penumbra region (in this study, the distance between the 90% and 10% relative doses), and (3) low-dose region. The acceptable dose difference in each region for the simple condition (without inhomogeneity or accessory) was 2% for the flat region, 10% for the penumbra region, and 30% for the low-dose region. In Venselaar *et al.*'s method, the percentage of the dose difference was expressed relative to the local point dose. These values for this study and the FWHM

values for the measurements and GATE for different field sizes are summarized in table 1. The profiles extracted from the measurements and simulations for the 6 × 6, 10 × 10 and 20 × 20 cm<sup>2</sup> field sizes are compared in figure 4.

**Table 1.** Dose differences and full width at half maximum (FWHM) values for transverse profiles of verification fields for Geant4 Application for Tomography Emission (GATE).

Field (cm)	Local dose difference			FWHM (mm)	
	Flat region	Penumbra	Low dose region	Measurement	GATE
6×6	0.1%	11.0%	18.1%	67.5	66.2
10×10	0.6%	10.2%	19.5%	110.6	110.0
20×20	0.6%	12.5%	17.1%	238.9	239.1

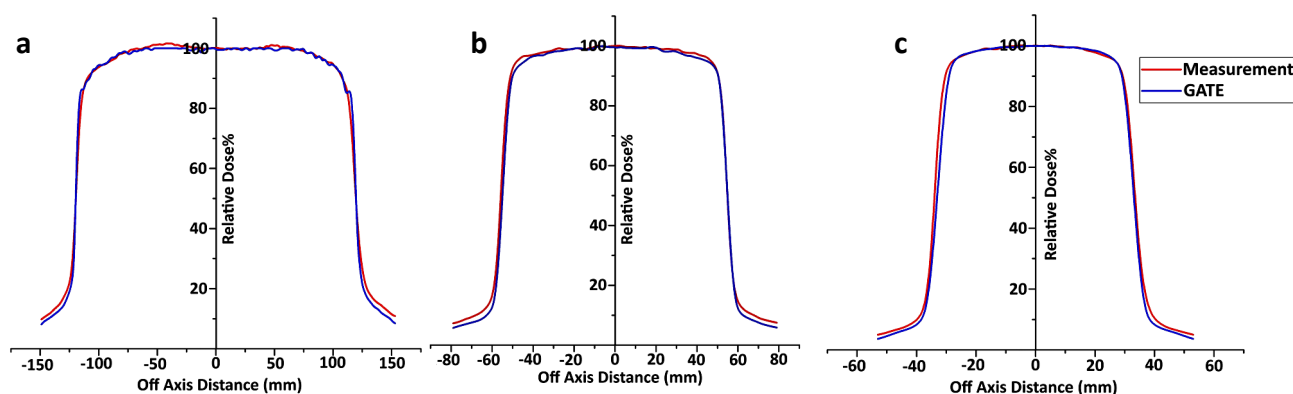


**Figure 4.** Comparison of transverse profiles between GATE simulations and measurements in (a) 6 × 6 cm<sup>2</sup>, (b) 10 × 10 cm<sup>2</sup>, and (c) 20 × 20 cm<sup>2</sup> field sizes.

### Comparison of the simulation with dose calculation algorithms

To discuss the simulation accuracy for the three patients, the mean dose difference between the CCC, CLKS, and CFFT algorithms and GATE simulations, differences in the brain region as the target tissue, and gamma pass rates for different dose calculation algorithms are presented in table 2. The PDDs obtained for the second patient are shown in figure 5. The comparison of transverse profiles was conducted in terms of the FWHM, which presents the definition of the dosimetric field size. The transverse profiles obtained for the second patient (as an example) are shown in figure 6, and the FWHM values for the three patients and all fields are presented in table 3. In addition, for the description of the statistical error in the MC approach, the ranges of relative statistical

uncertainties of the GATE output for any field along the central axis are presented in table 2.

### Comparison of the total output for a patient

A 3D view of the treatment plan in TPS for the second patient and a slice of its CT images with the irradiated beams are shown in figure 7(a) and figure 7(b), respectively. The total output of the GATE simulation code for this patient is graphically shown in figure 7(c), and the profiles and gamma indexes for the different dose calculation algorithms and GATE simulation in a central line are shown in figure 7(d). In addition, the gamma pass rates for the extracted data of the selected line for the CCC, CLKS, and CFFT algorithms as references compared with the GATE simulation output were 93.4%, 98.7%, and 96.0% respectively.

**Table 2.** Mean dose difference and gamma pass rate values for different dose calculation algorithms (collapsed cone convolution (CCC), convolution fast Fourier transform (CFFT), and Clarkson (CLKS)) compared with those from GATE simulations.

Patient No.	Field Angle	Mean difference in total curve of PDD			Mean difference in brain tissue region			Gamma pass rate with 3%/3mm criteria		
		CCC	CLKS	CFFT	CCC	CLKS	CFFT	CCC	CLKS	CFFT
Patient 1	90	2.0%	1.9%	2.6%	0.9%	1.5%	2.4%	92.4	93.9	89.4
	270	2.2%	3.0%	3.3%	1.1%	0.5%	2.2%	97.0	91.0	91.0
Patient 2	0	3.3%	3.2%	3.2%	1.9%	0.8%	1.4%	89.9	94.4	89.9
	90	2.8%	1.2%	1.3%	1.8%	0.9%	0.8%	97.4	93.6	94.9
	180	4.1%	3.9%	2.8%	2.9%	1.1%	1.3%	87.5	89.8	90.9
	270	2.4%	2.0%	2.2%	1.8%	0.9%	1.6%	94.7	96.0	97.3
Patient 3	60	2.6%	2.0%	4.1%	1.1%	1.0%	2.6%	93.8	90.8	93.8
	180	3.7%	1.8%	1.4%	3.6%	1.2%	0.9%	90.6	94.1	98.8
	300	2.2%	1.7%	2.9%	1.6%	1.1%	2.0%	91.7	90.0	90.0

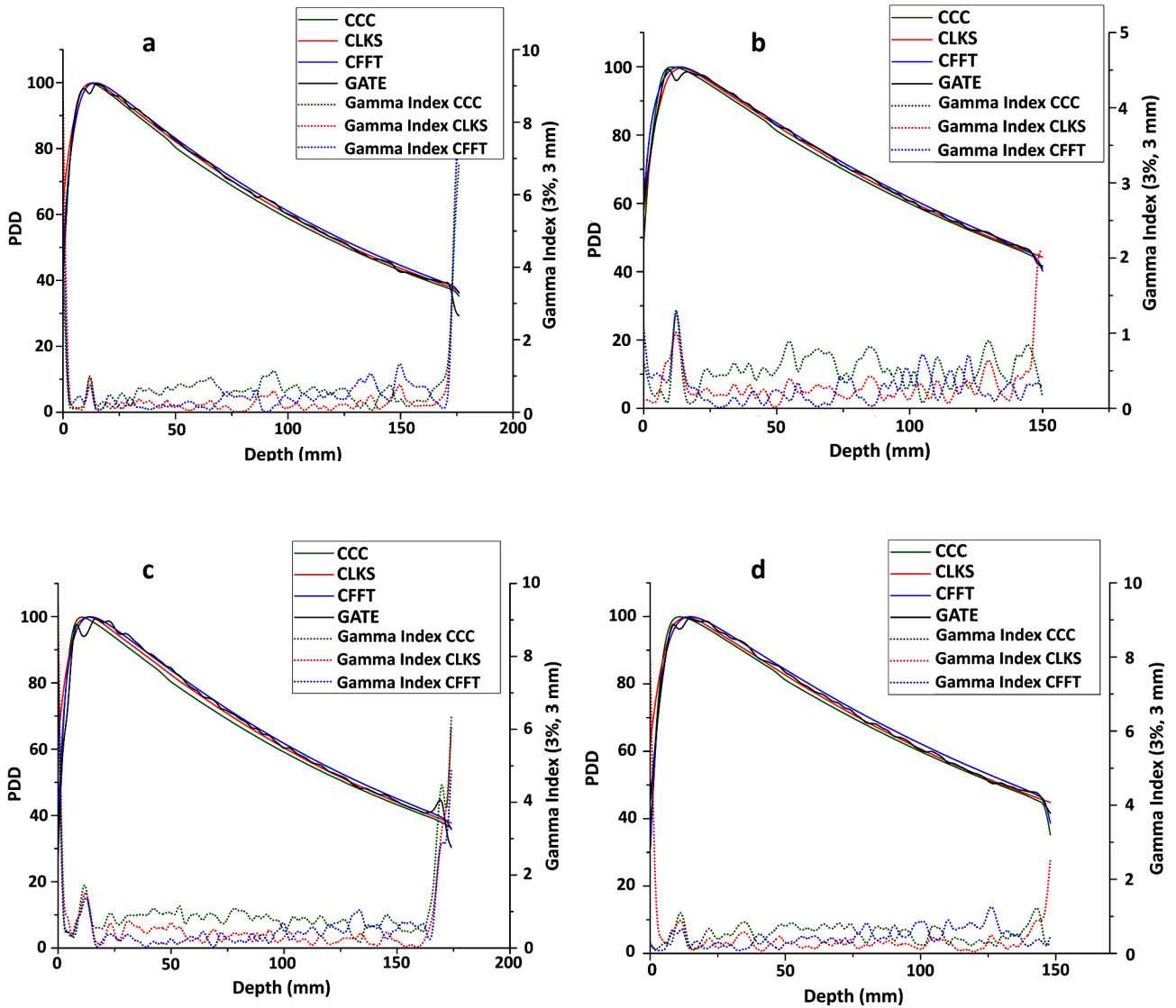


Figure 5. Comparison of PDDs and gamma evaluation between dose calculation algorithms and GATE simulation in the second patient for the field with angles of (a) 0°, (b) 90°, (c) 180°, and (d) 270°.

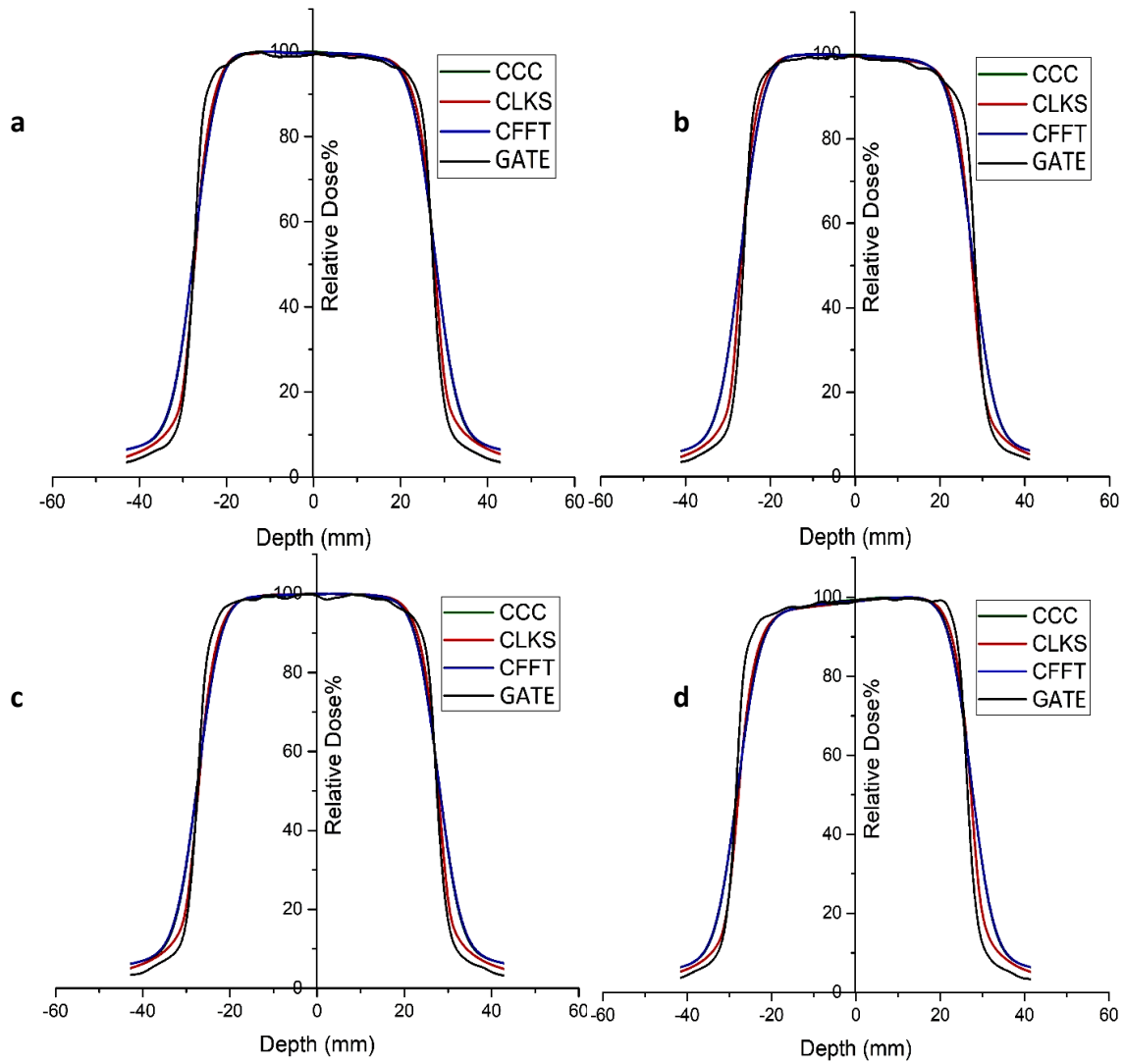


Figure 6. Comparison of transverse profiles between dose calculation algorithms and GATE simulations in the second patient for field with angles of (a) 0°, (b) 90°, (c) 180°, and (d) 270°.

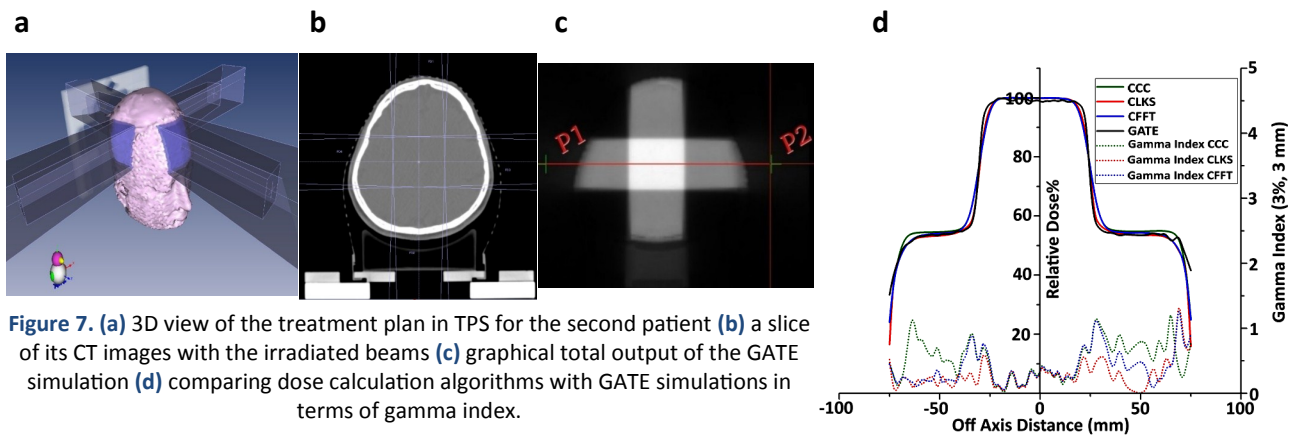


Figure 7. (a) 3D view of the treatment plan in TPS for the second patient (b) a slice of its CT images with the irradiated beams (c) graphical total output of the GATE simulation (d) comparing dose calculation algorithms with GATE simulations in terms of gamma index.

Table 3. FWHMs of all nine fields applied to three patients in the depth of isocenters.

Patient No.	Field sizes and angle	Depth of isocenter	Dose calculation method	FWHM (mm)	Difference between algorithms and simulation (mm)	Relative Error	Relative statistical uncertainty
Patient 1	4x4 cm <sup>2</sup> (90)	28 mm	CCC	39.1	0.1	0.3%	0.5-1%
			CLKS	39.6	0.6	1.7%	
			CFFT	39.1	0.1	0.3%	
			GATE	39.0	--	--	
	4x4 cm <sup>2</sup> (270)	104 mm	CCC	41.4	0.8	1.8%	0.5-1%
			CLKS	40.6	0.0	0.2%	
			CFFT	41.5	0.9	2.0%	
			GATE	40.6	--	--	
Patient 2	5.5x5.5 cm <sup>2</sup> (0)	94 mm	CCC	56.0	1.1	2.0%	0.8-1.2%
			CLKS	55.2	0.3	0.6%	
			CFFT	56.0	1.1	2.1%	
			GATE	54.9	--	--	
	5.5x5.5 cm <sup>2</sup> (90)	86 mm	CCC	55.3	0.7	1.2%	0.6-1.1%
			CLKS	54.7	0.1	0.1%	
			CFFT	55.3	0.7	1.1%	
			GATE	54.6	--	--	
	5.5x5.5 cm <sup>2</sup> (180)	72 mm	CCC	55.8	1.0	1.8%	0.7-1.1%
			CLKS	55.1	0.3	0.5%	
			CFFT	55.9	1.1	1.9%	
			GATE	54.8	--	--	
	5.5x5.5 cm <sup>2</sup> (270)	78 mm	CCC	56.0	1.2	2.1%	0.7-1.2%
			CLKS	55.2	0.4	0.7%	
			CFFT	56.0	1.2	2.1%	
			GATE	54.8	--	--	
Patient 3	5x6 cm <sup>2</sup> (60)	58 mm	CCC	49.7	0.3	0.6%	0.7-1.2%
			CLKS	48.3	1.1	2.3%	
			CFFT	49.8	0.4	0.7%	
			GATE	49.4	--	--	
	6x6 cm <sup>2</sup> (180)	76 mm	CCC	60.6	0.7	1.2%	0.6-1.1%
			CLKS	59.6	0.3	0.5%	
			CFFT	60.6	0.7	1.3%	
			GATE	59.9	--	--	
	7x6 cm <sup>2</sup> (300)	90 mm	CCC	71.7	0.7	1.0%	0.8-1.1%
			CLKS	70.4	0.6	0.8%	
			CFFT	71.7	0.7	1.0%	
			GATE	71.0	--	--	

## DISCUSSION

In this study, the performance of the GATE MC toolkit was investigated for external radiotherapy applications by comparing the results from water phantom measurements, three commercial TPS algorithms, and GATE simulations. The method utilized in this study was the insertion of the head CT images of the patients as a voxelized phantom in the GATE toolkit. This method helped to describe the patient's realistic geometry in the simulation and achieved a 3D matrix of the calculated dose. In the first step, the simulated dose was compared with measurements in the homogeneous water phantom for 10 × 10, 6 × 6 and 20 × 20 cm<sup>2</sup> field sizes to verify the GATE MC code. The mean dose differences were less than 1% for the 6 × 6 and 10 × 10 cm<sup>2</sup> field sizes and 1.3% for the 20 × 20 cm<sup>2</sup> field size, showing good agreement between the simulations and measurements. The maximum dose differences occurred in the buildup region, at 8.2%, 7.3%, and 12.8% for the 6 × 6, 10 × 10, and 20 × 20 cm<sup>2</sup> field sizes, respectively (figure 3). These differences were

due to a steep gradient of the dose distribution in the buildup region, which led to uncertainty in the ionization chamber measurements. Similar results were reported in another study<sup>(42)</sup>. As mentioned above, the beam profiles in the three regions were compared using the method recommended by Venselaar *et al.*<sup>(41)</sup>, and our results agree with those of their method. In addition, the results from our study are in good agreement with the results reported by Mesbahi *et al.*<sup>(42)</sup>. The PDDs of the simulation and measurement were assessed in terms of the gamma index. The field sizes of 6 × 6, 10 × 10 and 20 × 20 cm<sup>2</sup> had 100.0%, 98.4%, and 90.4% gamma pass rates, respectively, considering the 2%/2 mm criteria, indicating that more than 90% of the points were passed. This agrees with the study of Abolaban and Taha<sup>(18)</sup>, although they used 3%/3 mm criteria.

The primary purpose of this study was to evaluate the potency of the GATE toolkit in a rather complex simulation. For this purpose, the Isogray TPS containing three available algorithms (CCC, CLKS, and CFFT) was used. These algorithms were divided into

three groups based on the classifications proposed by Gershkevitch *et al.* <sup>(43)</sup> and Knoos *et al.* <sup>(44)</sup>. These three groups are: a) measurement-based algorithms (e.g., CLKS), b) model-based algorithms that cannot model changes in the lateral transport of the electrons (e.g., CFFT), and c) model-based algorithms that can model the changes in the lateral electron and photon transport (e.g., CCC).

Benhalouche *et al.* <sup>(35)</sup> evaluated and validated the GATE toolkit for Intensity-modulated Radiotherapy (IMRT) dosimetry. They evaluated the IMRT plan regarding absolute and relative doses for seven patient datasets using IMRT-dedicated quality assurance phantoms. For the IMRT plans, they found that the GATE simulation had good agreement with the measurements, and for all beams, they reported a gamma pass rate of  $90.8\% \pm 3.6\%$  with a 5%/4 mm criterion. This means that our results with the minimum gamma pass rate of 87.5% and the maximum gamma pass rate of 98.7% (overall gamma pass rate of 92.76%) by 3%/3 mm gamma criteria were in good agreement with the results of their study.

Grevillot *et al.* <sup>(49)</sup> assessed the GATE radiation therapy simulation tools by simulating the Elekta Precise 6 MV Linac. They compared simulations and measurements in a water phantom and reported good agreement between the simulations and measurements for depth doses and dose profiles, with dose differences of approximately 1% and 2%, respectively. Regarding the gamma index, they reported a more than 90% gamma pass rate with the 3%/3 mm criterion for all simulated cases. This indicates that our results corresponded with those from their study, but our results showed better agreement (gamma pass rate of 100% by 3%/3 mm criteria) between the simulations and measurements. It should be mentioned that they conducted their study by GATE v6.0, the older version of this platform. In another study, Tai *et al.* <sup>(45)</sup> compared dose distribution in acrylic phantom calculated by Panther TPS and the simulated in EGSnrc Monte Carlo in  $10 \times 10$  cm<sup>2</sup> field size and 90 cm SSD. They reported gamma pass rates of 98.7%, 96.4%, and 94.2% with 3%/3 mm, 2%/2 mm, and 1%/1 mm criteria, respectively, considering the 10% threshold of maximum dose. Furthermore, they compared PDDs and profiles of simulation and TPS in terms of gamma index and found good agreement between them, with gamma values less than 0.2 for almost all points. For  $10 \times 10$  cm<sup>2</sup> field size, we found gamma pass rates of 98.4% and 100% for 2%/2 mm and 3%/3 mm criteria, respectively. Also, we compared the results of GATE and measurements in  $6 \times 6$  and  $20 \times 20$  cm<sup>2</sup> field sizes and found good agreement with 100% and 90.4% gamma pass rates for 2%/2 mm criteria, respectively.

In this study, from comparing the PDDs, the majority of the discrepancies between the

simulations and TPS algorithms were observed in the buildup and end regions of the PDDs. In addition, the PDD extracted from the simulation, unlike that from the algorithms, shows two peaks in the entrance region and one peak on the other side of the head where photons must pass through interfaces (skin/bone/brain tissue). Sauer *et al.* <sup>(28)</sup> and Han *et al.* <sup>(29)</sup> reported that in the adjacency of interfaces between materials with different atomic compositions irradiated by photons, secondary electrons could create a nonequilibrium zone, and a local maximum and minimum could occur in the dose. All three algorithms in this study showed a disadvantage in calculating dose distributions in this region. Therefore, it is inferred that these algorithms cannot predict skull bones and have limitations in calculating the dose distributions at tissue interfaces with different atomic compositions (such as those of bone). For instance, Chow *et al.* <sup>(30)</sup> reported that the transport of primary electrons at the most profound depth is not considered complete because of using the density scaling method in CCC algorithms. Care must be taken for lung cancer patients with tumors near the chest wall; this drawback could be significant. <sup>(29)</sup>

The results showed that the dose differences in the brain tissue in all field sizes between the simulations and three dose calculation algorithms differed from 0.5% to 2.9% (under 3%), except for the  $6 \times 6$  cm<sup>2</sup> field for the third patient, which exceeded 3.6%. These results agree with those of other studies <sup>(29, 46)</sup>. As shown in figure 5, compared with the GATE, the CCC and CFFT algorithms underestimated and overestimated the dose, respectively, and the CLKS was more consonant in the brain tissue. The gamma pass rates with the 3%/3 mm criterion for the CCC, CLKS, and CFFT algorithms in all fields ranged from 87.5% to 97.4% (average 92.8%), 89.9% to 96.00% (average 92.6%), and 89.4% to 98.8% (average 92.9%), respectively. As presented in figure 7, a good agreement (more than 93% pass rate in the gamma index) was observed for the total output of the second patient between the simulation and algorithms. In the interface region, the gamma values showed additional discrepancies between the algorithms and simulations, as shown in figure 5. Benhalouche *et al.* <sup>(35)</sup> reported similar results ( $90.8\% \pm 3.6\%$  gamma pass rate), but they compared the dose distribution using the planar gamma index, with a 5%/4 mm criterion. Najafzadeh *et al.* <sup>(25)</sup> evaluated the CCC dose calculation accuracy by comparing it with the BEAMnrc MC code and measurements in terms of the 3D gamma index in a lung phantom. In the Planning Target Volume (PTV), right lung, lung-tissue interface, and spinal cord volumes, the gamma pass rates with 2%/2 mm criteria were 59%, 83.06%, 76.97%, and 83.08%, those with 3%/3 mm criteria were 83.0%, 87.5%, 77.3%, and 88.6%, and those with 5%/5 mm criteria

were 97.5%, 93.7%, 78.7%, and 93.2%, respectively. It can be seen that the results of our study are more accurate for the 3%/3 mm criteria, but it must be considered that their phantom was more inhomogeneous. Also, Tai *et al.* (45) compared the dose distribution of 15 Jaw-Only IMRT (J-O IMRT) of nasopharyngeal patients calculated by MC and the CCC algorithm. The average gamma pass rates of  $93.3 \pm 3.1\%$ ,  $92.8 \pm 3.2\%$ , and  $92.4 \pm 3.4\%$  with 3%/3 mm, 2%/2 mm, and 1%/1 mm criteria were reported which with considering 92.8% average gamma pass rate for CCC algorithm in our work the closeness of both studies results can be seen.

Some studies have investigated other algorithms, such as Acuros XB (AXB), compared with MC codes that do not fall into the stated categories, and they presented better results in heterogeneous regions (29, 44, 47). Acuros XB is a grid-based Boltzmann equation solver algorithm whose dose calculation accuracy in the heterogeneous and interface regions is comparable to that of the MC method. Han *et al.* (29) compared the AXB algorithm implemented in Eclipse TPS with EGSnrc MC simulations, an Anisotropic Analytical Algorithm (AAA), and CCC. Their comparison was made in water as a homogenous phantom and in a multilayer slab phantom containing soft tissue, bone, and lung. They found that the AXB algorithm had results closer to those of the MC relative to those of AAA and CCC for all plans, especially in the bone and lung regions, and had better dose calculations at the tissue interfaces. We did not compute the dose differences in the head organs individually, but it can be observed from the PDDs and gamma histogram figure (figure 5) that all three algorithms, in contrast to the GATE simulation, could not predict the dose distributions at tissue interfaces correctly. The GATE simulation can provide a better view of the GATE potential for dose predictions in heterogeneous regions, especially at tissue interfaces, in which many algorithms have limitations regarding dose calculations.

The FWHM values of the transverse profiles were compared for the simulations and dose calculation algorithms (figure 7). The relative error percentage and absolute difference of the calculated FWHM for the CCC, CLKS, and CFFT algorithms compared to the GATE simulation ranged from 0.3% to 2.1% (0.1 to 1.2 mm), 0.1% to 2.3% (0.1 to 1.1 mm), and 0.3% to 2.1% (0.1 to 1.2 mm), respectively. All the simulated fields in the GATE code agreed well with those of the dose calculation algorithms and were very close to the predefined field sizes.

## CONCLUSION

Regarding the dose difference and gamma index, the GATE met the desired criteria, and in terms of the FWHM, it had good agreement with both the TPS algorithms and the prescribed field sizes. Most of the

dose differences between the simulations and dose calculation algorithms were observed in the bone-brain tissue interface, owing to the limitations of the dose calculation algorithms. Hence, it was concluded that the utilized dose calculation algorithms had less accuracy than the GATE code in this work, especially in the tissue interfaces and the surface of the phantom. This study shows that the GATE toolkit can be implemented for radiotherapy dose calculations.

## ACKNOWLEDGMENTS

*This article was derived from the M.Sc. thesis of the first author. Also, the authors would like to appreciate the support from all staff of the radiotherapy center of Emam Hossein hospital.*

**Conflict of interest:** The authors declare that there is no conflict of interest.

**Data availability statement:** The data that support the findings of this study are available from the corresponding author upon reasonable request.

**Author Contribution:** All authors contributed equally to this study, data curation and analysis, and the writing of the manuscript. All authors read and approved the final manuscript.

**Funding:** This research did not receive any specific grant from funding agencies.

**Ethical considerations:** <http://ethics.research.ac.ir/IR.SBMU.MSP.REC.1398.584>

**Approval date:** 2019-09-24

## REFERENCES

- Sarrut D, Bardies M, Bousson N, *et al.* (2014) A review of the use and potential of the GATE Monte Carlo simulation code for radiation therapy and dosimetry applications. *Med Phys*, **41**(6): 064301.
- Papadimitroulas P (2017) Dosimetry applications in GATE Monte Carlo toolkit. *Phys Med*, **41**: 136-140.
- Slimani FAA, Hamdi M, Bentourkia MH (2018) G4DARI: Geant4/GATE based Monte Carlo simulation interface for dosimetry calculation in radiotherapy. *Comput Med Imaging Graph*, **67**: 30-39.
- Krieger T and Sauer OA (2005) Monte Carlo-versus pencil-beam/collapsed-cone-dose calculation in a heterogeneous multi-layer phantom. *Phys Med Biol*, **50**(5): 859-68.
- Zaman A, Kakakhel MB, Hussain A (2019) A comparison of Monte Carlo, anisotropic analytical algorithm (AAA) and Acuros XB algorithms in assessing dosimetric perturbations during enhanced dynamic wedged radiotherapy deliveries in heterogeneous media. *J Radiother Pract*, **18**(1): 75-81.
- Lee B, Jeong S, Chung K, *et al.* (2019) Feasibility of a GATE Monte Carlo platform in a clinical pretreatment QA system for VMAT treatment plans using TrueBeam with an HD120 multileaf collimator. *J Appl Clin Med Phys*, **20**(10): 101-10.
- Nahum AE (1999) Condensed-history Monte-Carlo simulation for charged particles: what can it do for us? *Radiat Environ Biophys*, **38**(3): 163-173.
- Andreo P (1991) Monte Carlo techniques in medical radiation physics. *Phys Med Biol*, **36**(7): 861.
- Nahum A (2007) Monte-Carlo based patient dose computation. Handbook of Radiotherapy Physics: Theory and Practice. Taylor & Francis, Inglaterra.
- Mostaar A, Alahverdi M, Shahriari M (2003) Application of MCNP4C Monte Carlo code in radiation dosimetry in heterogeneous phantom. *Int J Radiat Res*, **1**: 143-149.
- Elcim Y, Dirican B, Yavas O (2018) Dosimetric comparison of pencil beam and Monte Carlo algorithms in conformal lung radiotherapy. *J Appl Clin Med Phys*, **19**(5): 616-624.

12. Thiam C O, Breton V, Donnarieix D, et al. (2008) Validation of a dose deposited by low-energy photons using GATE/GEANT4. *Phys Med Biol*, **53**(11): 3039-55.
13. Visvikisa D, Bardiesb M, Chiavassab S, et al. (2006) Use of the GATE Monte Carlo package for dosimetry applications. *Nucl*, **569**(2): 335-340.
14. Brualla L, Rodriguez M, Lallena AM (2017) Monte Carlo systems used for treatment planning and dose verification. *Strahlenther Onkol*, **193**(4): 243-259.
15. Byrnes K, Ford A, Bennie N (2019) Verification of the Elekta Monaco TPS Monte Carlo in modelling radiation transmission through metals in a water equivalent phantom. *Phys Eng Sci Med*, **42**(2): 639-45.
16. Santin G, Strul D, Lazaro D, et al. (2003) GATE: A Geant4-based simulation platform for PET and SPECT integrating movement and time management. *IEEE Trans Nucl Sci*, **50**(5): 1516-1521.
17. Jan S, Santin G, Strul D, et al. (2004) GATE: a simulation toolkit for PET and SPECT. *Phys Med Biol*, **49**(19): 4543-61.
18. Abolaban FA and Taha EM (2020) Representation and illustration of the initial parameters in GATE 8.1 Monte Carlo simulation of an Elekta Versa-HD linear accelerator. *J Radiat Res Appl Sc*, **13**(1): 642-7.
19. Grévillot L, Frisson T, Maneval D, et al. (2011) Simulation of a 6 MV Elekta Precise Linac photon beam using GATE/GEANT4. *Phys Med Biol*, **56**(4): 903-18.
20. Jan S, Benoit D, Becheva E, et al. (2011) GATE V6: a major enhancement of the GATE simulation platform enabling modelling of CT and radiotherapy. *Phys Med Biol*, **56**(4): 881-901.
21. GATE (2017) GATE User's Guide Version: GATE 8.0. OpenGATE Collaboration <http://www.opengatecollaboration.org/UsersGuide/>; March 2017
22. Shalek RJ (1977) Determination of absorbed dose in a patient irradiated by beams of X or gamma rays in radiotherapy procedures. *Med Phys*, **4**(5): 461.
23. Hasenbalg F, Neuenschwander H, Mini R, Born EJ (2007) Collapsed cone convolution and analytical anisotropic algorithm dose calculations compared to VMC++ Monte Carlo simulations in clinical cases. *Phys Med Biol*, **52**(13): 3679-369.
24. Reis QM, Nicolucci P, Fortes SS, Silva LP (2019) Effects of heterogeneities in dose distributions under nonreference conditions: Monte Carlo simulation vs dose calculation algorithms. *Med Dosim*, **44**(1): 74-82.
25. Najafzadeh M, Nickfarjam A, Jabbari K, et al. (2019) Dosimetric verification of lung phantom calculated by collapsed cone convolution: A Monte Carlo and experimental evaluation. *J Xray Sci Technol*, **27**(1): 161-175.
26. Yavuzkanat N and Kürem HBS (2020) Monte Carlo Simulation of the Gamma-Ray Transmissions for the newly Designed Shielding Blocks used in Radiotherapy. *J Adv Res*, **6**(2): 364-77.
27. Aspradakis MM (1997) A study to assess and improve dose computations in photon beam therapy. *Med Phys*, **24**(8): 1334-1334.
28. Sauer OA (1995) Calculation of dose distributions in the vicinity of High-Z interfaces for photon beams. *Med Phys*, **22**(10): 1685-1690.
29. Han T, Mikell J K, Salehpour M, Mourtada F (2011) Dosimetric comparison of Acuros XB deterministic radiation transport method with Monte Carlo and model-based convolution methods in heterogeneous media. *Med Phys*, **38**(5): 2651-2664.
30. Chow J C, Leung M K, Van Dyk J (2009) Variations of lung density and geometry on inhomogeneity correction algorithms: A Monte Carlo dosimetric evaluation. *Med Phys*, **36**(8): 3619-3630.
31. Fogliata A, Vanetti E, Albers D, et al. (2007) On the dosimetric behaviour of photon dose calculation algorithms in the presence of simple geometric heterogeneities: comparison with Monte Carlo calculations. *Phys Med Biol*, **52**(5): 1363-1385.
32. Schneider W, Bortfeld T, Schlegel W (2000) Correlation between CT numbers and tissue parameters needed for Monte Carlo simulations of clinical dose distributions. *Phys Med Biol*, **45**(2): 459-78.
33. Vanderstraeten B, Chin PW, Fix M, et al. (2007) Conversion of CT numbers into tissue parameters for Monte Carlo dose calculations: a multi-centre study. *Phys Med Biol*, **52**(3): 539-62.
34. Kawrakow I and Walters B (2006) Efficient photon beam dose calculations using DOSXYZnrc with BEAMnrc. *Med Phys*, **33**(8): 3046-3056.
35. Benhalouche S, Visvikis D, Le Maitre A, et al. (2013) Evaluation of clinical IMRT treatment planning using the GATE Monte Carlo simulation platform for absolute and relative dose calculations. *Med Phys*, **40**(2): 021711.
36. Seroul P, Sarrut D (2008) VV: a viewer for the evaluation of 4D image registration, presented at Medical Image Computing and Computer-Assisted Intervention MICCAI Workshop
37. Palmans H, Andreo P, Huq MS, et al. (2017) Dosimetry of small static fields used in external beam radiotherapy: an IAEA-AAPM international code of practice for reference and relative dose determination. *Med Phys*, **45**(11): e1123-e45.
38. Low DA, Harms WB, Mutic S, Purdy JA (1998) A technique for the quantitative evaluation of dose distributions. *Med Phys*, **25**(5): 656-661.
39. Hussein M, Clark C, Nisbet A (2017) Challenges in calculation of the gamma index in radiotherapy—towards good practice. *Phys Med*, **36**: 1-11.
40. Williams T, Kelley C Gnuplot software (ver 4.4.3). Web access (preferred): <https://sourceforge.net/projects/gnuplot>
41. Venselaar J, Welleweerd H, Mijnheer B (2001) Tolerances for the accuracy of photon beam dose calculations of treatment planning systems. *Radiother Oncol*, **60**(2): 191-201.
42. Mesbahi A, Reilly A J, Thwaites D I (2006) Development and commissioning of a Monte Carlo photon beam model for Varian Clinac 2100EX linear accelerator. *Appl Radiat Isot*, **64**(6): 656-662.
43. Gershkevitch E, Schmidt R, Velez G, et al. (2008) Dosimetric verification of radiotherapy treatment planning systems: Results of IAEA pilot study. *Radiother Oncol*, **89**(3): 338-346.
44. Knöös T, Wieslander E, Cozzi L, et al. (2006) Comparison of dose calculation algorithms for treatment planning in external photon beam therapy for clinical situations. *Phys Med Biol*, **51**(22): 5785-807.
45. Tai DT, Oanh LT, Son ND, et al. (2019) Dosimetric and Monte Carlo verification of jaws-only IMRT plans calculated by the Collapsed Cone Convolution algorithm for head and neck cancers. *Rep Pract Oncol*, **24**(1): 105-114.
46. Chopra KL, Leo P, Kabat Ch, et al. (2018) Evaluation of dose calculation accuracy of treatment planning systems in the presence of tissue heterogeneities. *Ther Radiol Oncol*, **2**: 28.
47. Stathakis S, Esquivel C, Vazquez Quino L, et al. (2012) Accuracy of the small field dosimetry using the Acuros XB dose calculation algorithm within and beyond heterogeneous media for 6 MV photon beams. *Int J Med Phys Clin Eng Radiat Oncol*, **1**: 78-87.

